Radiation Physics and Chemistry 226 (2025) 112247

Contents lists available at ScienceDirect

Radiation Physics and Chemistry

journal homepage: www.elsevier.com/locate/radphyschem

Application of INTDOSKIT tool for assessment of uncertainties on dose coefficients for ingestion of uranium by workers

Thomas Makumbi [a,*], Bastian Breustedt [b], Wolfgang Raskob [a], Sadeeb Simon Ottenburger [a]

[a] Institute for Thermal Energy Technology and Safety (ITES), Karlsruhe Institute of Technology (KIT), Hermann-von-Helmholtz Platz 1, 76344, Eggenstein-Leopoldshafen, Germany
[b] Institute of Biomedical Engineering (IBT), Karlsruhe Institute of Technology (KIT), Kaiserstraße 12, 76131, Karlsruhe, Germany

ARTICLE INFO

Handling Editor: Dr. Chris Chantler

Keywords:
INTDOSKIT
Uncertainty analysis
Sensitivity analysis
Uranium
Ingestion

ABSTRACT

The International Commission on Radiological Protection (ICRP) has developed the Human Alimentary Tract Model (HATM) to calculate radiation doses from the ingestion of radionuclides for the protection of workers and the public. In parallel, the ICRP's Occupational Intake of Radionuclides (OIR) series provides biokinetic models and dose coefficients based on a reference human, primarily for regulatory purposes. Although these coefficients are not usually checked for uncertainties, the investigation of such uncertainties is crucial to ensure their reliability in radiation protection. This study uses INTDOSKIT, a software tool developed using the R programming language and RStudio as the Integrated Development Environment (IDE), to calculate doses and explore uncertainties following ingestion of U-238 by workers. Two scenarios were investigated: Case I, using the latest HATM model and the systemic uranium model from ICRP publications 100 and 137 respectively, and Case II, based on data from literature, using older ICRP models. In both cases, intake of U-238 in its soluble form (Type F) was modeled and the results were validated using the ICRP OIR dataviewer software. Following validation, uncertainty and sensitivity analyses were performed. In Case I, uncertainties were assigned to the particle transport parameters in both the systemic model model and HATM as well as the uranium uptake fraction into the blood. While in Case II they were limited to the uptake fraction (f_1) and the systemic uranium model. A Monte Carlo simulation of 60,000 runs was performed for both cases, sampling model parameters from their respective probability distributions to generate dose distributions. The influence of each parameter on these distributions was also analyzed. Probability distributions were inferred to the calculated dose values using the maximum likelihood estimation method and the Kolmogorov-Smirnov goodness-of-fit. The results showed that for both cases the committed effective dose coefficient, e (50), followed a lognormal distribution. Case I had a geometric mean of 3.2E-08 Sv/Bq and GSD of 2.0, while case II had a slightly lower geometric mean of 3.1E-08 Sv/Bq and GSD of 1.9. Sensitivity analysis showed that the main contributor to dose uncertainty was the fraction of uranium absorbed from the small intestine into the blood. Both cases showed similar trends, with slightly higher results in case I. Overall, this study demonstrates the effectiveness of INTDOSKIT in calculating dose coefficients and analyzing uncertainties. It suggests that while the ICRP reference values remain useful for protection, the incorporation of additional statistical measures and distribution characteristics could further enhance radiation protection strategies.

1. Introduction

Uranium is an actinide element that occurs primarily in oxidation states IV and VI (ICRP, 2017). There are about 22 known isotopes of uranium, but only 3 isotopes, namely U-234, U-235, and U-238, have relative mass abundances in undisturbed crustal rocks of 0.005, 0.72, and 99.275% respectively (Li et al., 2005; Agha et al., 2011). Uranium occurs in industry in various physical and chemical forms, including oxides, inorganic salts, and some organic compounds (ICRP, 2017). Some forms, particularly metal, carbide and oxide, can be depleted (~0.2% U-235), natural (0.7% U-235) or enriched (>0.7% U-235) (ICRP, 2017; Rump et al., 2019).

Studies of occupational uranium intake have provided direct evidence of human carcinogenicity (Kreuzer et al., 2015). Occupational

* Corresponding author.
E-mail address: thomas.makumbi@kit.edu (T. Makumbi).

https://doi.org/10.1016/j.radphyschem.2024.112247
Received 7 May 2024; Received in revised form 20 August 2024; Accepted 16 September 2024
Available online 18 September 2024

exposure to uranium occurs primarily through the intake of the naturally occurring isotopes U-238 and U-234, which are mainly ingested through food and drinking water (Ma et al., 2020). U-235 is not considered a significant radiation hazard compared to U-238 due to its lower abundance in natural rocks (Rump et al., 2019; Lopez et al., 2020). Although the annual doses to workers from uranium are much lower than those from radon progeny, uranium doses remain a significant radiation protection concern due to their association with the nuclear fuel cycle (Marsh et al., 2012; Puncher and Burt, 2013).

In its OIR series (ICRP, 2017, 2019, 2022), ICRP has published dose coefficients for internal emitters incorporated into the body. To assess radiation doses, models are required to simulate the external exposure geometry, the biokinetics of the incorporated radionuclides and the human body. The reference models and the necessary reference parameters are established and selected from a number of experimental investigations and human data. However, there are uncertainties in their derivation and application that should be investigated in order to assess the reliability of these dose coefficients when used as protective quantities in radiation protection. Uncertainty analysis is therefore considered to be a useful tool for quantifying sources of uncertainty in model systems and has been applied to the calculation of uncertainties in internal doses from radionuclide intake (Puncher and Harrison, 2012).

Over the past decades, several authors have conducted studies on the uncertainty analysis of doses from the ingestion of actinides. For example, Puncher and Burt (2013) evaluated the reliability of dose coefficients for the inhalation and ingestion of uranium by the public in the United Kingdom. These authors derived the uncertainties in the parameter values of the biokinetic model to calculate the distribution of the effective dose per unit intake, using the ICRP publication 60 formalism (ICRP, 1991). They expressed the uncertainties in the derived dose distributions using uncertainty factors (UF). However, in their study, Puncher and Burt (2013) did not consider the dose from progeny and the uncertainty in particle transport rates within the gastrointestinal tract (GIT).

Puncher and Harrison (2012) on the other hand performed an uncertainty analysis of doses from acute ingestion of plutonium and americium by the public. However, these elements have different biokinetics in the human body than uranium (ICRP, 2015). Additionally, their study used the GIT model from ICRP Publication 30 (ICRP, 1979) to model the ingestion process, and the study was conducted for members of the public.

This paper describes the use of INTDOSKIT, an in-house software tool developed in R using RStudio as the integrated development environment (IDE), to perform a parameter uncertainty analysis of doses from uranium ingestion by workers under two scenarios. Case I involved the use of the latest systemic model of uranium (ICRP, 2017) and the Human Alimentary Tract Model (HATM) (ICRP, 2006), including consideration of progeny doses. Case II used the systemic model of uranium published in ICRP publication 69 (ICRP, 1995) and the GIT model of ICRP publication 30 (ICRP, 1979), without consideration of progeny doses. The purpose of the study was therefore twofold: first, to demonstrate the capability of INTDOSKIT, and second, to perform uncertainty and sensitivity studies using the most recent information available on occupational intakes and thereafter compare the results for both scenarios. For detailed information on INTDOSKIT, which applies the ICRP internal dosimetry methodology, interested readers are referred to Breustedt et al. (2024).

2. Materials and methods

2.1. Biokinetic models

The latest systemic model structure describing the biological and physiological processes of uranium in the human body after absorption into the blood was published by ICRP in its publication 137 (ICRP, 2017). This structure reflects similarities in the biokinetics of uranyl (UO^{2+}) and calcium (Ca^{2+}) ions and is similar to the generic structure developed for alkaline earth elements (Puncher and Burt, 2013). The interested reader is referred to ICRP publication 137 for further information on the biokinetics of uranium in systemic organs.

In case I, the HATM model described in ICRP publication 100 (ICRP, 2006) was used to model the biokinetics and dosimetry of uranium in the alimentary tract. This model provides a more realistic physiological representation of the material in the alimentary tract and replaces the previously used gastrointestinal tract (GIT) model (Li et al., 2009). The most important parameter in the HATM is the fraction of ingested material (f_A) entering blood from the alimentary tract. This fraction represents the amount of ingested material that is absorbed from the alimentary tract into the blood and is an indicator of how much of the ingested material reaches the systemic organs and tissues of the human body. However, often, as in the case of uranium, information on regional absorption of radionuclides is not available, and the default assumption is that all absorption takes place in the small intestine (ICRP, 2006). The interested reader is referred to ICRP publication 100 (ICRP, 2006) for more detailed information on the HATM.

For Case II, the ICRP publication 30 GIT model was used to model the biokinetics of uranium in the gastrointestinal tract. The most important parameter in the ICRP publication 30 GIT model is the fraction (f_1) of uranium absorbed from GIT to blood (ICRP, 1979; Li, 2018). The overall biokinetic model structure used in this study for occupational ingestion of uranium involves a combination of the two biokinetic models, i.e., the systemic model and the HATM/GIT were combined via the pathways representing the transfer of material from the contents of the small intestine to the blood and the excretion of material from the blood to the right colon contents/upper large intestine contents, as shown in Figs. 1 and 2 for Case I and Case II respectively.

2.2. Assignment of probability distributions to model parameters

2.2.1. Probability distributions for the systemic model parameters

The probability distributions for the systemic model of uranium were taken from the work of Puncher and Burt (2013). This is because the behavior of a given element in the human body is the same for all its isotopes (ICRP, 2015, 2017). These authors conducted an analysis of the data set available in the literature and derived probability distributions for the transfer rates in the systemic model of uranium. In their analysis, they performed a local sensitivity analysis of the effective dose per unit uranium intake, in addition to considering the weighted organ doses that contribute most to the effective dose. Puncher and Burt (2013), then selected probability distributions such that the medians of the simulated bioassay prediction distributions were as close as possible to those calculated using the ICRP reference values at various times after ingestion. The derived probability distributions are presented in Table 1.

2.2.2. Probability distributions for the HATM parameters

The fraction of the radionuclide absorbed from the alimentary tract (f_A) is the most important parameter for ingested intake (ICRP, 2006). This is because for many radionuclides, uncertainties in the effective dose are directly proportional to uncertainties in f_A, since the effective dose is largely affected by the irradiation of organs and tissues due to the absorption of activity in the blood (ICRP, 2006; Li, 2018). This parameter depends on the ingested chemical form and mass of the element, individual diet, nutritional status, and numerous physiological parameters such as age, sex, and health status of the subject (ICRP, 2006; Puncher and Burt, 2013).

The probability distribution for this parameter, assuming a lognormal distribution with a median equal to the ICRP value (0.02) and a GSD of 1.6, was taken from Puncher and Burt (2013). This distribution was assumed to represent the uncertainty in the population means according to Puncher and Burt (2013). For particle transport within the HATM, distributions describing uncertainties in transfer rates were taken from Kwon et al. (2020), who derived transfer rate probability

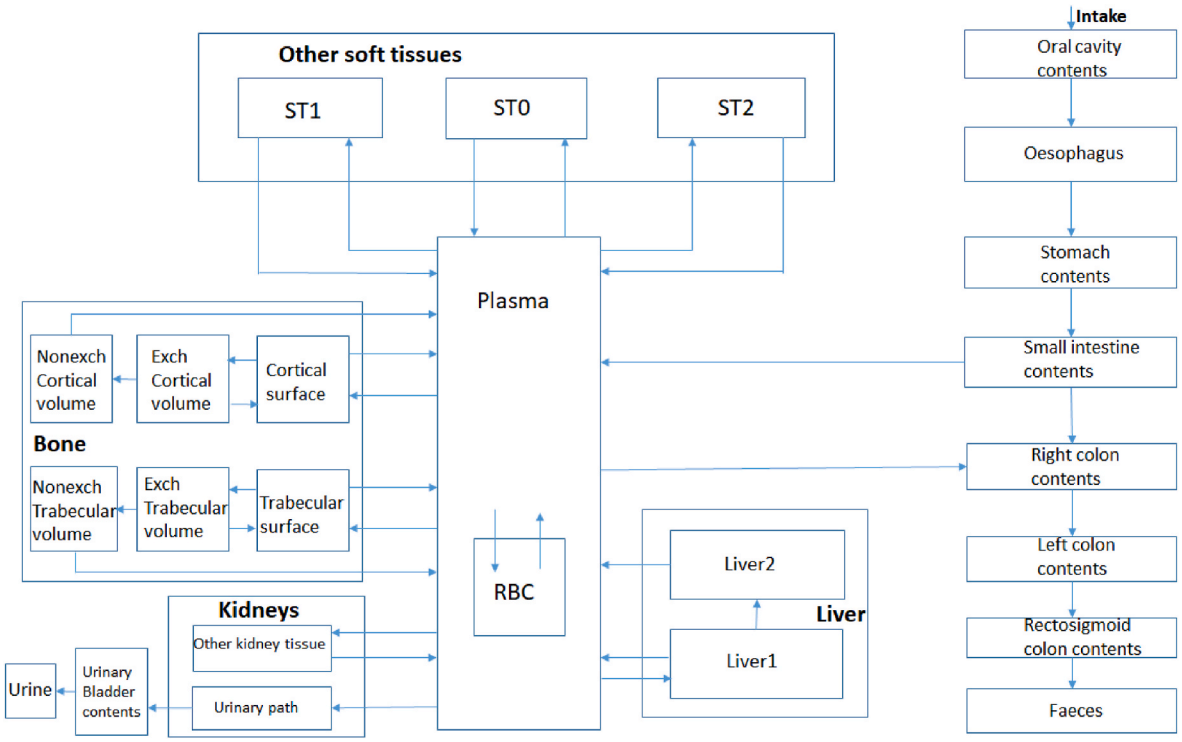

Fig. 1. Biokinetic model for ingestion of uranium using ICRP 137 and ICRP 100 HATM (Case I).

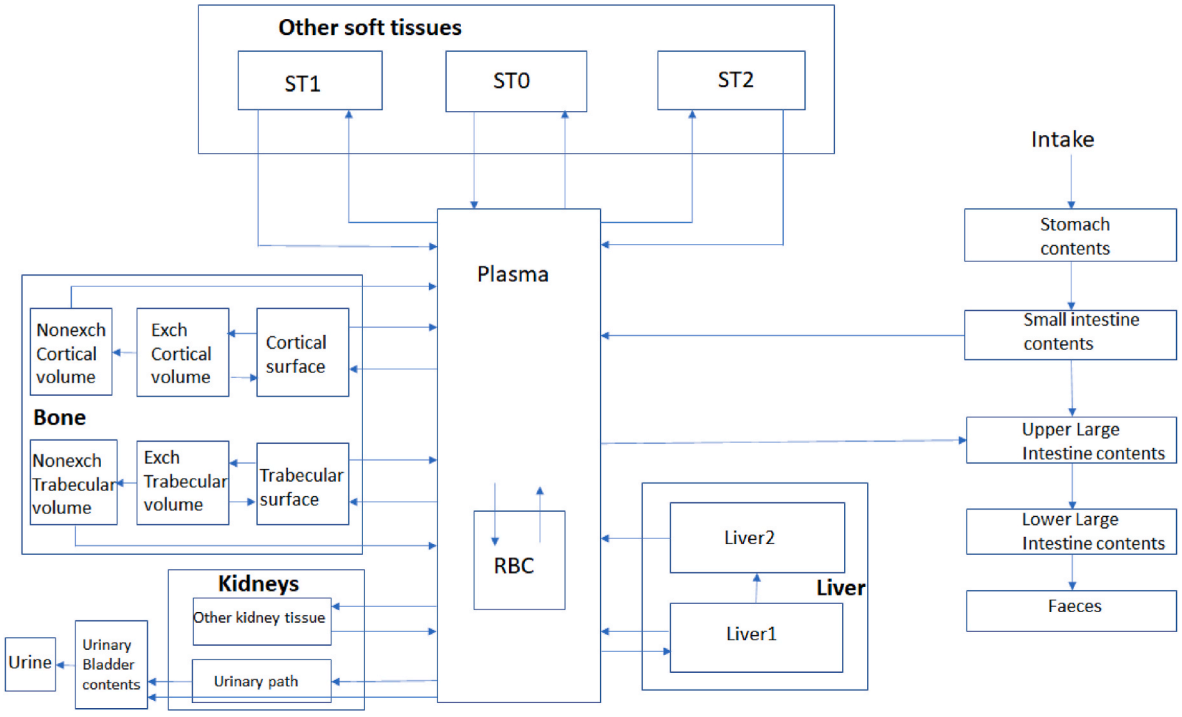

Fig. 2. Biokinetic model structure for ingestion of uranium using ICRP 69 and ICRP 30 GIT model (Case II).

distributions from the uncertainty factors UF proposed by Leggett et al. (2007). The study by Kwon et al. (2020) assumed lognormal distributions with the median equal the ICRP reference value. Table 2 shows these probability distributions.

2.3. Dose calculations for the ingestion of U-238

The biokinetics and dosimetry of U-238 uptake were modeled using the INTDOSKIT software tool. INTDOSKIT was the preferred choice for this work because other available software tools require a commercial license, which is costly. Additionally, many of these tools only perform dose calculations and it is impossible to perform uncertainty and

Table 1
Probability distributions derived for the systemic model of uranium.

From	To	Distribution	GM[a]	GSD[b]	Remarks[c]
Blood	CS/TS	Lognormal	1.00	1.30	Correlated
CS/TS	Other	Lognormal	1.00	1.30	Correlated
ECV/ETV	Other	Lognormal	1.00	1.41	Correlated
NECV/NETV	Other	Lognormal	1.00	1.41	Correlated
Blood	UBC	Lognormal	1.00	1.73	Correlated
Blood	ST2	Lognormal	ICRP[d]	1.73	Uncorrelated
Blood	Liver1	Lognormal	ICRP[d]	1.41	Uncorrelated

CS: Cortical bone surface; TS: Trabecular bone surface; ECV: Exchangeable Cortical bone volume; ETV: Exchangeable Trabecular bone volume; NECV: Nonexchangeable Cortical bone volume; NETV: Nonexchangeable Trabecular bone volume; UBC: Urinary bladder contents; ST2: Soft tissues with long term retention.

[a] Geometric mean for a lognormal probability distribution.

[b] Geometric standard deviation for a lognormal probability distribution.

[c] All rates for correlated parameters were varied together above and below the reference value. This regime was implemented by varying rates together using a common factor sampled from a lognormal distribution with a median of unity and given geometric standard deviation (GSD). For the uncorrelated parameters, the rate was varied by assuming the parameter follows a lognormal distribution with the median equal to the ICRP reference value and given GSD.

[d] Reference value for the parameter was obtained from ICRP Publication 137 (ICRP, 2017) for Case I and ICRP Publication 69 (ICRP, 1995) for Case II.

Table 2
Probability distributions for the transfer rates in the HATM.

From	To	Distribution	GM[c]	GSD[d]
Oral-cavity	Oesophagus-fast	Lognormal	6480	1.52[a]
Oral-cavity	Oesophagus-slow	Lognormal	720	1.52[a]
Oesophagus-fast	Stomach	Lognormal	12343	1.52[a]
Oesophagus-slow	Stomach	Lognormal	2160	1.52[a]
Stomach	Small-intestine	Lognormal	20.57	1.28[b]
Small-intestine	Right-colon	Lognormal	6.00	1.28[b]
Right-colon	Left-colon	Lognormal	2.00	1.28[b]
Left-colon	Rectosigmoid-colon	Lognormal	2.00	1.28[b]
Rectosigmoid-colon	Faeces	Lognormal	2.00	1.28[b]

[a] Derived from the proposed UF of 2 for the 95% confidence interval.

[b] Derived from the proposed UF of 1.5 for the 95% confidence interval.

[c] Geometric mean for the lognormal probability distribution.

[d] Geometric standard deviation for the lognormal distribution.

sensitivity studies with these tools. Finally, INTDOSKIT is able to take advantage of the statistical and graphical capabilities of the R programming language to perform statistical analysis on the generated posterior distributions. Basing on the above arguments, the authors decided to use an in-house tool that could be easily adapted to the task at hand. The detailed description of the use of INTDOSKIT to model the biokinetics and dosimetry of decay chains has been described elsewhere (Breustedt et al., 2024).

Using INTDOSKIT, the parameters of the reference man were used to calculate the committed dose coefficients. In solving the model for Case I, the authors implemented the entire U-238 decay chain down to the last stable nuclide, Pb-206. However, upon critical analysis of the retention data and calculated doses, the authors observed that the total dose is mainly contributed by the first three nuclides in the chain (U-238, Th-234, and Pa-234). Therefore, a decision was taken to truncate the chain after Pa-234 to save computer memory and calculation time. For Case II, only the parent nuclide (U-238) was considered in the calculations with no consideration to progeny. The calculated committed dose coefficients were later validated against data from the ICRP OIR data viewer software (ICRP, 2022). The ICRP reference dose calculation methodology used in this work is presented in Fig. 3.

2.4. Monte Carlo methods for uncertainty and sensitivity analysis

Upon successful validation of the model (see results below), Monte Carlo simulations were performed with INTDOSKIT. These Monte Carlo calculations were based on a random sample of 60,000 runs implemented in the code to ensure convergence. Dose values were calculated for each matrix of sampled values following ingestion of 1 Bq of U-238. For each run, the following steps were implemented in the code.

i) The parameters of interest were sampled from their respective probability distributions. For parameters not assigned probability distributions, ICRP default (reference) values were assumed. This set of parameters was then used to generate a matrix of transfer coefficients that was used in solving the biokinetic model.
ii) The matrix generated in step (i) was then propagated directly into the solution of the biokinetic model to generate a vector of the number of decays in each compartment of the biokinetic model for an intake of 1 Bq of U-238, which were then assigned to the ICRP dosimetric source regions.
iii) The numbers of decays from step (ii) were used in the dosimetric model to calculate the equivalent organ dose coefficients and the effective dose coefficients for a committed period of 50 years using the ICRP radiation and tissue weighting factors.
iv) Steps (i) - (iii) were repeated for each of the 60,000 runs and a dose distribution was obtained. The calculated dose values were stored in a text file for further processing (statistical analysis).

Fig. 4 presents the Monte Carlo simulation concept that was used in this work.

Determining the number of iterations required is the main challenge in Monte Carlo simulations with random sampling. In this paper, a central limit theorem approach was used to determine the number of iterations required. The central limit theorem states that the mean of a sample is normally distributed regardless of the type of distribution of the data from which the sample was drawn. However, this is only true if the size of the population is significantly larger than the sample size (Heijungs, 2020). The number of iterations required for the Monte Carlo simulations was therefore determined as follows;

The Monte Carlo simulation was performed with a reasonable number of runs. In this case, 500 runs and a standard deviation was obtained for the resulting dose distribution. The number 500 was chosen because, based on the authors' experience, this sample size would meet the criteria for sample standard deviation and convergence. Secondly, it was necessary to choose a number that would not take too long to run the model, but would be large enough for the sample standard deviation

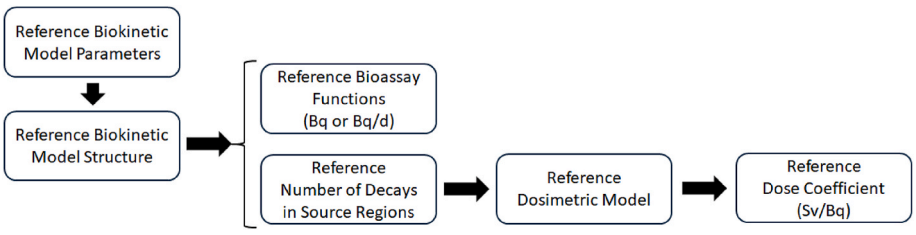

Fig. 3. ICRP methodology for internal dose calculation.

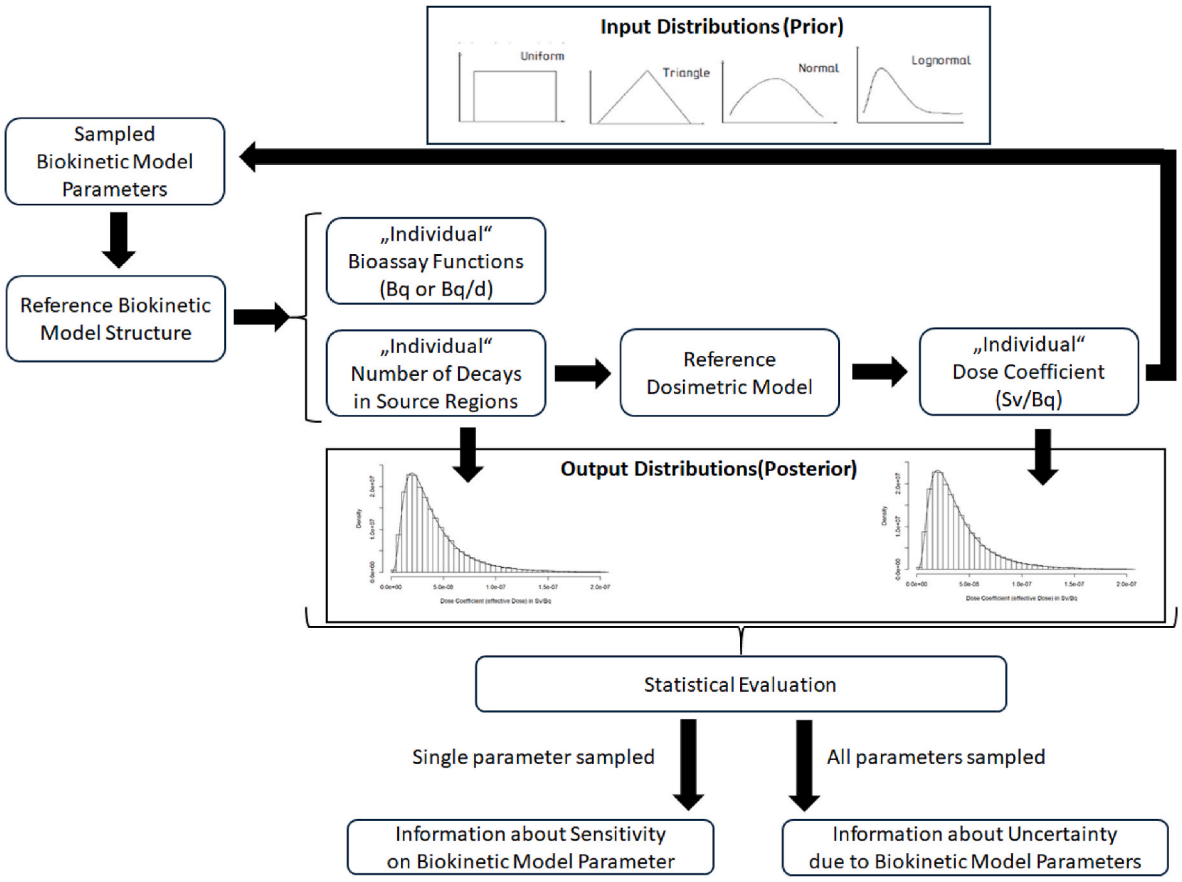

Fig. 4. Monte Carlo method for uncertainty and sensitivity studies used in this work.

to converge reasonably well. This was accomplished as follows.

i) The first step was to select the desired confidence level and associated z-statistic. In this case, it was the 95% confidence level with 1.96 as the associated z-statistic.
ii) The second step was to solve equation (1) for the number of iterations, n.

$$z = (\bar{x} - \mu) / (s / \sqrt{n}) \ldots\ldots\ldots \quad (1)$$

Where $\bar{x} - \mu$ is the desired level of precision i.e., 0.01 in this case, s is the sample standard deviation, n is the required number of iterations and z is the chosen z-statistic.

Having determined the required number of iterations, the simulation was repeated approximately n times to achieve the desired accuracy.

2.5. Sensitivity of doses to uncertainty on the amount of uranium absorbed to blood from the alimentary tract

To assess the relative contribution of the variability of the systemic parameters and the f_A parameter to the overall uncertainty in the calculated dose, additional Monte Carlo simulations were performed. For this purpose, the Monte Carlo approach was repeated with the following modifications.

i) The particle transport parameters were varied, but the f_A value was fixed at the ICRP reference value.
ii) The particle transport parameters were fixed at their ICRP reference values, but the f_A value was varied.

2.6. Sensitivity of doses to variation in rates governing turnover of uranium in bone

The distributions assumed to represent the variation in the rate of uranium loss from bone surfaces and bone volume were largely based on expert judgement. Given the large uncertainties associated with the rate of uranium removal from bone surfaces, further Monte Carlo simulations were performed as follows.

i) The particle transport parameters were varied but the f_A value was fixed at the ICRP reference value.
ii) The particle transport parameters were varied but the f_A value was fixed at the ICRP reference value and the rates from bone surface to bone volume were fixed at their reference values.
iii) All parameter values were fixed at their reference values but the rates from bone surface and bone volume were varied.

2.7. Sensitivity of doses to variation in HATM rates

The distributions assumed to represent the variation in the rate of uranium transfer were applied here. In order to investigate their contribution to the overall uncertainty in the calculated committed effective dose coefficient, further Monte Carlo simulations were performed as follows.

i) The particle transport parameters including HATM rates were varied but the f_A value was fixed at the ICRP reference value.
ii) The particle transport parameters were varied but the f_A value was fixed at the ICRP reference value and the HATM rates were fixed at their reference values.

iii) All parameter values were fixed at their reference values but the HATM rates were varied.

2.8. Fitting a probability distribution to the generated posterior data set

A probability distribution was fitted to the posterior data set in INTDOSKIT using maximum likelihood estimation (MLE) and the Kolmogorov-Smirnov (K–S) test. The functions to accomplish this task can be found under the fitdistrplus library of R.

3. Results and discussions

3.1. Dose calculations for the ingestion of U-238

The results of the committed dose coefficients calculations and validation are presented in Table 3, where they are compared with the data from the ICRP OIR dataviewer software. The results presented in Table 3 show that INTDOSKIT is a reliable tool for modeling decay chains. The INTDOSKIT calculations for Case I are in close agreement with the ICRP data, with a maximum deviation of 4% while a maximum deviation of (−8%) was obtained for Case II. This slightly higher deviation for Case II emphasizes the importance of considering the contribution of progeny to the total dose calculations for more accurate and reliable results. The organs receiving the highest doses in both cases are the liver, kidneys, bone surfaces and bone marrow. For Case I, the relative contribution of each radionuclide to the total effective dose coefficient over a 50-year exposure period, e (50), is also shown in Table 4. The percentage deviation of the calculated values for both males and females were calculated using equation (2);

$$Percentage\ deviation = \left(\frac{Calculated\ value - ICRP\ value}{ICRP\ value}\right) x100 \ldots\ldots\ldots\ldots \quad (2)$$

Table 4
Relative contribution of each nuclide to the total effective dose coefficient (Sv/Bq).

Nuclide	e (50)	Contribution (%)
U-238	3.00E-08	97.34
Th-234	3.15E-11	0.10
Pa-234	7.88E-10	2.56
U-234	2.86E-13	0.00
Th-230	1.79E-16	0.00
Ra-226	7.87E-20	0.00
Rn-222	8.43E-21	0.00
Po-218	1.03E-20	0.00
Pb-214	1.17E-21	0.00
Bi-214	6.32E-21	0.00
Po-214	1.81E-20	0.00
Pb-210	4.34E-24	0.00
Bi-210	2.56E-22	0.00
Po-210	3.53E-21	0.00
Total	3.08E-08	100.00

Table 4 shows that the first three radionuclides in the U-238 chain contribute significantly to the total committed effective dose coefficient. Therefore, in the Monte Carlo simulations for uncertainty and sensitivity analysis, the authors decided to end the chain after Pa-234 to save computational time and memory, since the contributions from the lower nuclides were negligible.

3.2. Uncertainty on doses from ingestion

The convergence of the final dataset with 60,000 repetitions was tested by calculating the GSD of the distribution of committed effective dose coefficient after every 500th run. Fig. 5 shows the GSD of the distribution against the number of repetitions. As expected, the values of the first 20,000 runs show a larger fluctuation with values ranging from 1.964 to 2.003. After 25,000 runs the fluctuations are within ±0.2% of

Table 3
Dose coefficients (Sv/Bq) for ingestion of 1 Bq of U-238 using reference man parameters.

Organ/Tissue	Case I		ICRP (2022)		Case II		Deviation (%) [c]		Deviation (%) [d]	
	Male	**Female**	**Male**	**Female**	**Male**	**Female**	**Male**	**Female**	**Male**	**Female**
Bone Marrow	3.9E-08	4.5E-08	3.8E-08	4.6E-08	3.5E-08	4.3E-08	2	−2	−8	−7
Colon	1.9E-08	2.4E-08	1.9E-08	2.4E-08	1.9E-08	2.4E-08	0	0	0	0
Lung	1.5E-08	1.8E-08	1.5E-08	1.8E-08	1.5E-08	1.8E-08	0	0	0	0
Stomach	2.0E-08	2.4E-08	2.0E-08	2.4E-08	2.0E-08	2.5E-08	0	0	0	4
Breast	2.4E-08	2.9E-08	2.4E-08	2.9E-08	2.4E-08	2.9E-08	0	0	0	0
Gonads[a]	2.4E-08	2.5E-08	2.4E-08	2.4E-08	2.4E-08	2.4E-08	0	2	0	0
Urinary Bladder	2.5E-08	3.0E-08	2.5E-08	2.9E-08	2.5E-08	3.0E-08	0	3	0	3
Oesophagus	2.0E-08	2.5E-08	2.0E-08	2.4E-08	2.0E-08	2.4E-08	0	3	0	0
Liver	7.3E-08	9.6E-08	7.3E-08	9.5E-08	7.2E-08	9.4E-08	0	1	−1	−1
Thyroid	2.2E-08	2.7E-08	2.2E-08	2.6E-08	2.2E-08	2.6E-08	0	3	0	0
Bone Surface	1.4E-07	1.6E-07	1.4E-07	1.6E-07	1.3E-07	1.5E-07	0	0	−7	−6
Brain	2.5E-08	3.0E-08	2.5E-08	2.9E-08	2.4E-08	2.9E-08	0	3	−4	0
Salivary glands	2.4E-08	3.0E-08	2.4E-08	2.9E-08	2.4E-08	2.9E-08	0	3	0	0
Skin	2.4E-08	3.5E-08	2.4E-08	3.5E-08	2.4E-08	3.5E-08	0	0	0	0
Adrenals	2.1E-08	2.6E-08	2.1E-08	2.5E-08	2.1E-08	2.6E-08	0	4	0	4
Gall bladder	2.4E-08	3.0E-08	2.4E-08	2.9E-08	2.4E-08	2.9E-08	0	3	0	0
Heart	2.2E-08	2.6E-08	2.2E-08	2.6E-08	2.2E-08	2.6E-08	0	0	0	0
Kidneys	1.9E-07	2.2E-07	1.9E-07	2.2E-07	1.9E-07	2.2E-07	0	0	0	0
Muscle	2.5E-08	3.0E-08	2.5E-08	2.9E-08	2.5E-08	3.0E-08	0	3	0	3
Oral Mucosa	2.6E-08	3.2E-08	2.6E-08	3.1E-08	2.5E-08	3.0E-08	0	3	−4	−3
Pancreas	2.1E-08	2.5E-08	2.1E-08	2.5E-08	2.1E-08	2.5E-08	0	0	0	0
Prostate	2.4E-08	0	2.4E-08	0	2.4E-08	0	0	0	0	0
Small Intestine	1.9E-08	2.4E-08	1.9E-08	2.4E-08	1.9E-08	2.4E-08	0	0	0	0
Spleen	1.7E-08	2.2E-08	1.7E-08	2.1E-08	1.7E-08	2.1E-08	0	4	0	0
Thymus	2.4E-08	3.0E-08	2.4E-08	2.9E-08	2.4E-08	2.9E-08	0	3	0	0
Uterus	0	2.9E-08	0	2.9E-08	0	2.9E-08	0	0	0	0
e (50)[b]	3.1E-08		3.1E-08		3.0E-08		0		−3	

[a] Gonads represent testes and ovaries for male and female respectively.
[b] e (50) represents the committed effective dose coefficient (Sv/Bq) for a committed period of 50 years.
[c] Percentage deviation of the Case I value against that obtained from ICRP OIR dataviewer (ICRP, 2022).
[d] Percentage deviation of the Case II value against that from ICRP OIR dataviewer (ICRP, 2022).

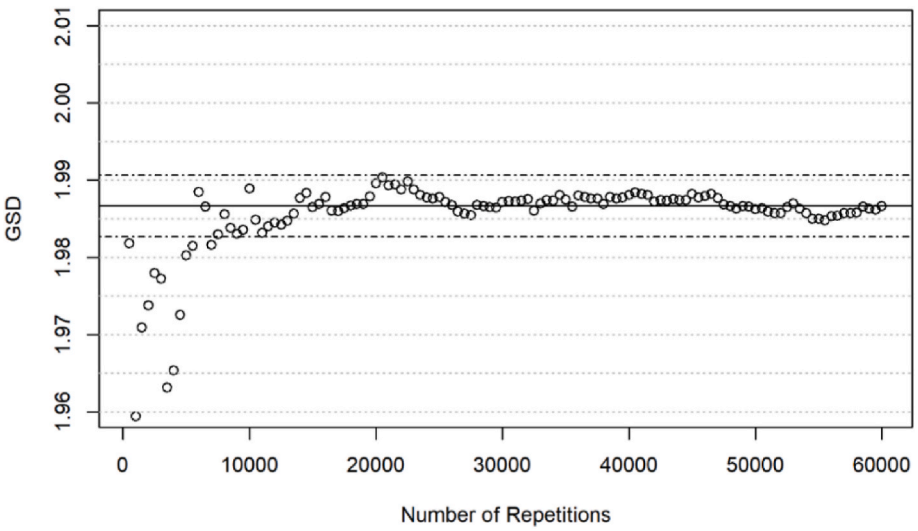

Fig. 5. Test for convergence of the dataset. The x-axis gives the number of repetitions and the y-axis shows the GSD of the distribution of the dose coefficient for effective dose. The solid line gives the final GSD of the whole dataset of 60,000 repetitions, dash dotted lines indicate ±0.2% range around this value.

Table 5
Statistical summary of results from uncertainty analysis of e (50) (Sv/Bq) for the ingestion of U-238.

	All parameters	
	Case I[b]	**Case II**[c]
ICRP value[a]	3.1E-08	3.1E-08
Mean	4.0E-08	3.8E-08
Median	3.2E-08	3.1E-08
GSD	2.0	1.9
Q_L	8.4E-09	8.5E-09
Q_U	1.2E-07	1.1E-07
Mean/ICRP	1.3	1.2
Median/ICRP	1.0	1.0
Q_U/ICRP	3.9	3.6
ICRP/Q_L	3.7	3.6

GSD: Geometric standard deviation; Q_U: the upper 97.5th percentile; Q_L: the lower 2.5th percentile.

[a] Value taken from ICRP OIR dataviewer (ICRP, 2022).

[b] Study implemented in INTDOSKIT with variation of HATM rates and inclusion of progeny.

[c] Study implemented in INTDOSKIT using the data obtained from Puncher and Burt (2013).

the GSD value of the dataset of 1.98529.

A statistical summary of the effective dose per unit intake of U-238 given in Table 5 shows that the mean committed effective dose coefficient is 1.3 times higher than the ICRP reference value, indicating an average increase of 30%. The median is consistent with the ICRP reference, indicating that the central tendency is in agreement with the ICRP estimate. The upper bound of the simulated dose coefficient is significantly higher, indicating significant uncertainty at the upper end, while the lower bound shows less, but still significant uncertainty at the lower end. However, the elevated mean indicates a positive skewness in the lognormal distribution used for the model parameters.

Skewness means that higher values in the distribution pull the mean upward, indicating an asymmetry with more frequent larger dose values than a normal distribution would suggest. This highlights the influence of extreme values on the mean. The wide range of uncertainty (from Q_L to Q_U) of about two orders of magnitude reflects significant variability in the dose coefficients due to model parameter uncertainties. This suggests that for conservative safety assessments it may be prudent to consider values higher than the ICRP reference.

The conclusion is that while the ICRP reference value can still be used as a protective measure, incorporating additional statistical measures and considering distributional characteristics could enhance protection. Adjustments to the reference value based on higher percentiles (e.g., 75th or 95th), adopting the mean as the reference value, or revising model parameters to reduce skewness could lead to more comprehensive and protective radiation protection measures.

The distribution of the committed effective dose coefficient, e (50) was well fitted by a lognormal distribution with a geometric mean of 3.2E-08 Sv/Bq and a geometric standard deviation (GSD) of 2.0 for Case I (see Fig. 6) while that of Case II was well fitted with a lognormal distribution with a geometric mean of 3.1E-08 Sv/Bq and GSD of 1.9 (see Fig. 7). This fit was accepted with a Kolmogorov-Smirnov (K–S) statistic of 0.00522, indicating a maximum difference between the empirical cumulative distribution function (CDF) of the data and the CDF of the fitted distribution of 0.00522. This value, which is below the critical value of 0.01, indicates an excellent fit.

The K–S test was chosen because of its nonparametric nature, sensitivity to distribution differences, applicability to different sample sizes, ease of interpretation, uniform distribution of test statistics, and versatility in testing different distributions (Aslam, 2019; Lanzante, 2021; Cardoso and Galeno, 2023). Other tests, such as the Chi-square goodness-of-fit test, the Anderson-Darling test, and the Shapiro-Wilk method, were inappropriate because of their specific limitations with small sample sizes, specificity for normal distributions, and inefficiencies in handling continuous data (Surucu, 2008; Ghasemi and

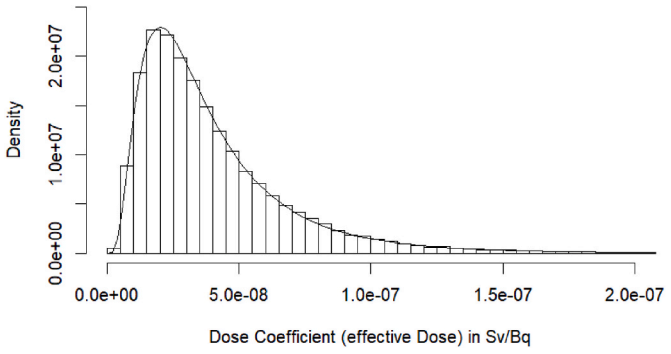

Fig. 6. Density plot of the distribution of the committed effective dose coefficient following ingestion intake of U-238. The histogram shows the dataset, the line is the fit of a lognormal distribution with geometric mean of 3.2E-08 Sv/Bq and GSD of 2.0 to the dataset.

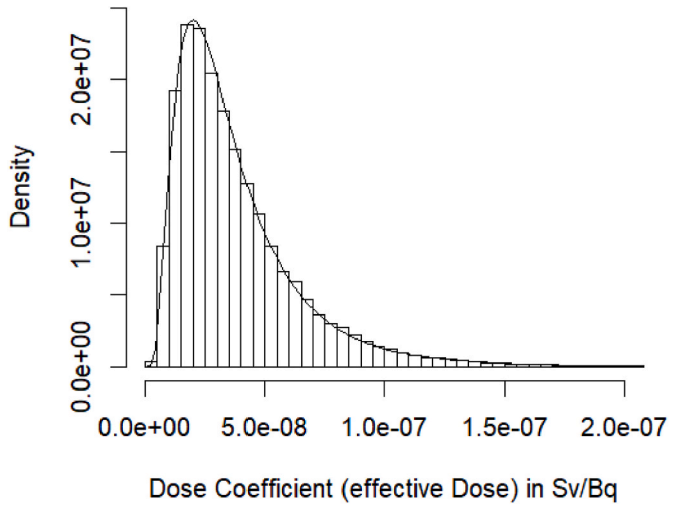

Fig. 7. Density plot of the distribution of the committed effective dose coefficient following ingestion intake of U-238 using the model of Puncher and Burt (2013). The histogram shows the dataset, the line is the fit of the lognormal distribution with geometric mean of 3.1E-08 Sv/Bq and GSD of 1.9.

Zahediasl, 2012; Rana and Singhal, 2015; Luong, 2018; Khatun, 2021; Hagel et al., 2024).

From Table 5, the GSD of the distribution obtained in Case I also agrees well with that obtained in other studies (Puncher and Burt, 2013), although the UF is 1.1 times higher than that obtained by Puncher and Burt (2013). This difference in UF can be explained by the fact that in their study, Puncher and Burt used the GIT model published in ICRP Publication 30, while in this study, the most recent model published in ICRP Publication 100 was used.

Additionally, Puncher and Burt (2013) only considered the variation of the f_1 parameter (parameter and particle transport rates in the systemic model) in their uncertainty analysis while in this study (Case I), both the variation of the f_A parameter and particle transport rates for both the systemic model and the HATM were implemented. Lastly, Puncher and Burt (2013) did not consider the contribution of the progeny to the total dose in their study, while in this study, the authors decided to include the progeny even though the progeny contributes a very small fraction (about 2.5%) to the total dose. For comparison purposes, it was necessary to model the scenario of Puncher and Burt (2013) (Case II) to get an idea of the effect of progeny and uncertainty in the HATM rates on the calculated committed dose coefficients. The results are presented in Fig. 7 and Table 5.

Boxplots for the distributions of committed effective dose and equivalent dose coefficients to the organs and tissues for Case I are shown in Fig. 8. The statistical parameters of the distributions are compiled in Table 6. From Table 6, the biggest uncertainties occur in the breast, testes and skin (GSD = 2.14; UF = 4.43) while the least uncertainties occur in the remainder tissues (GSD = 1.94, UF = 3.66). Similar trends were also noted for Case II as shown in Table 7. Therefore, UF for the organs and tissues range from 3.66 to 4.43 while the GSD values range from 1.94 to 2.14.

Tables 6 and 7 give the statistical summary of the committed equivalent dose coefficients (nSv/Bq) of various organs and tissues from the ingestion of U-238 for Case I and Case II respectively. These values are derived from an uncertainty analysis using INTDOSKIT, with comparisons to ICRP reference values.

In Case I, the mean committed equivalent dose coefficients for most organs are higher than the ICRP reference values, with ratios ranging from 1.24 to 1.40. The median committed dose coefficients are closer to the ICRP values, with most organs having ratios of about 0.99–1.02, indicating that although the average dose is higher, the typical (median) dose is quite similar to the ICRP values. Simulation results for Case II show that the median committed equivalent dose coefficients are also generally higher than the ICRP values, with ratios ranging from 1.19 to 1.32. The mean committed dose coefficients are also close to the ICRP values compared to Case I, with ratios ranging from approximately 0.98 to 1.01.

The GSD values are consistently around 2.08 to 2.14 for most organs in both analyses, indicating a similar degree of variability in the dose distributions. These high GSD values suggest a lognormal distribution of the committed dose coefficients with significant variability. In Case I, the 2.5th percentile (Q_L) and the 97.5th percentile (Q_U) show a wide range, reflecting the uncertainty and variability in the dose estimates. The Q_U/ICRP ratios are significantly high (around 3.64 to 4.32), indicating that the upper end of the committed dose coefficients distributions can be much higher than the ICRP reference values. On the other hand, the ICRP/Q_L ratios (3.62–4.43) show that the lower end of the dose distribution is also significantly lower than the ICRP values.

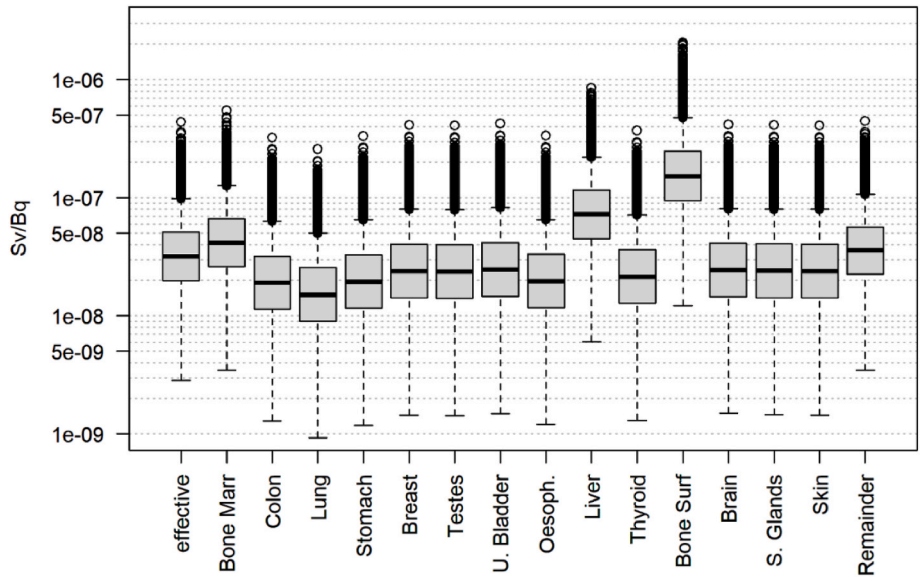

Fig. 8. Boxplots of the distributions of the dose coefficients for committed effective and equivalent dose coefficients to the organs following ingestion of U-238 for Case I scenario.

Table 6
Statistical summary of equivalent dose coefficients (nSv/Bq) from the uncertainty analysis of organ and tissue doses for the ingestion of U-238 under Case I.

Parameter	BM	CL	LG	ST	BR	TE	UB	OS	LV	TD	BS	BN	SG	SK	RM
ICRP	38.70	19.30	15.30	19.70	24.30	24.00	24.90	19.90	73.30	21.80	140.00	24.60	24.30	24.20	35.20
Mean	52.10	25.40	20.10	26.00	32.00	31.60	32.80	26.20	90.90	28.70	196.00	32.40	32.10	31.90	44.50
Median	41.80	19.10	15.10	19.50	24.00	23.80	24.70	19.70	73.00	21.60	153.00	24.40	24.10	23.90	35.90
GSD	1.97	2.12	2.13	2.13	2.14	2.14	2.14	2.13	1.97	2.13	2.03	2.13	2.13	2.14	1.94
Q_L	11.00	4.48	3.48	4.47	5.48	5.42	5.63	4.53	19.20	4.93	38.50	5.59	5.51	5.46	9.73
Q_U	153.00	82.60	65.50	84.90	105.00	103.00	107.00	85.40	267.00	94.00	603.00	106.00	105.00	104.00	129.00
Mean/ICRP	1.35	1.32	1.31	1.32	1.32	1.32	1.32	1.32	1.24	1.32	1.40	1.32	1.32	1.32	1.26
Median/ICRP	1.08	0.99	0.99	0.99	0.99	0.99	0.99	0.99	1.00	0.99	1.09	0.99	0.99	0.99	1.02
Q_U/ICRP	3.95	4.28	4.28	4.31	4.32	4.29	4.30	4.29	3.64	4.31	4.31	4.31	4.32	4.30	3.66
ICRP/Q_L	3.52	4.31	4.40	4.41	4.43	4.43	4.42	4.39	3.82	4.42	3.64	4.40	4.41	4.43	3.62

BM: Bone marrow; CL: Colon; LG: Lung; ST: Stomach; BR: Breast; TE: Testes; UB: Urinary bladder; OS: Oesophagus; LV: Liver; TD: Thyroid; BS: Bone surface; BN: Brain; SG: Salivary glands; SK: Skin; RM: Remainder.
GSD: Geometric standard deviation; Q_U: the upper 97.5th percentile; Q_L: the lower 2.5th percentile.

Table 7
Statistical summary of equivalent dose coefficients (nSv/Bq) from the uncertainty analysis of organ and tissue doses for the ingestion of U-238 under Case II.

Parameter	BM	CL	LG	ST	BR	TE	UB	OS	LV	TD	BS	BN	SG	SK	RM
ICRP	38.70	19.30	15.30	19.70	24.30	24.00	24.90	19.90	73.30	21.80	140.00	24.60	24.30	24.20	35.20
Mean	45.86	24.61	19.46	25.33	31.21	30.77	32.03	25.31	87.16	28.02	184.19	31.23	31.11	31.06	43.00
Median	37.55	18.95	14.99	19.50	24.00	23.66	24.63	19.48	71.48	21.55	146.80	24.01	23.92	23.88	35.46
GSD	1.94	2.08	2.08	2.08	2.08	2.08	2.08	2.08	1.91	2.08	1.98	2.08	2.08	2.08	1.89
Q_L	10.31	4.52	3.58	4.64	5.70	5.62	5.85	4.64	20.07	5.13	38.95	5.70	5.68	5.67	10.23
Q_U	129.42	77.77	61.47	80.09	98.79	97.40	101.37	80.04	246.48	88.67	546.09	98.84	98.48	98.31	120.09
Mean/ICRP	1.19	1.28	1.27	1.29	1.28	1.28	1.29	1.27	1.19	1.29	1.32	1.27	1.28	1.28	1.22
Median/ICRP	0.97	0.98	0.98	0.99	0.99	0.99	0.99	0.98	0.98	0.99	1.05	0.98	0.98	0.99	1.01
Q_U/ICRP	3.34	4.03	4.02	4.07	4.07	4.06	4.07	4.02	3.36	4.07	3.90	4.02	4.05	4.06	3.41
ICRP/Q_L	3.75	4.27	4.27	4.25	4.26	4.27	4.26	4.29	3.65	4.25	3.59	4.32	4.28	4.27	3.44

BM: Bone marrow; CL: Colon; LG: Lung; ST: Stomach; BR: Breast; TE: Testes; UB: Urinary bladder; OS: Oesophagus; LV: Liver; TD: Thyroid; BS: Bone surface; BN: Brain; SG: Salivary glands; SK: Skin; RM: Remainder.
GSD: Geometric standard deviation; Q_U: the upper 97.5th percentile; Q_L: the lower 2.5th percentile.

The mean/ICRP ratios for most organs are around 1.32, indicating that the doses for Case I are on average about 32% higher than the ICRP reference values while the median/ICRP ratios are around 0.99, indicating that the typical dose is very close to the ICRP values, highlighting a skewed distribution with a long tail on the higher dose side. In contrast, results from Case II show slightly lower mean/ICRP ratios (around 1.27), indicating that the average dose factor is about 27% higher than the ICRP values. The median/ICRP ratios are close to 0.98 which is consistent with Case I, indicating that the mean committed dose coefficients are quite similar to the ICRP values.

Both studies indicate that the mean committed dose coefficients are higher than the ICRP reference values suggesting that the average risk may be underestimated by the ICRP reference values. The median doses being close to ICRP values suggest that for the typical person, the ICRP values are a reasonable estimate. The high GSD values reflect substantial variability in dose estimates, emphasizing the need for considering individual variability in radiological protection. The significant differences in the upper and lower percentiles (Q_U and Q_L) compared to the ICRP values indicate that while typical doses are well represented by ICRP values, the extremes (both high and low) are not. This suggests potential underestimation of risk in scenarios involving high exposure.

3.3. Sensitivity of dose to uncertainty on the fraction of uranium absorbed from the alimentary tract to blood

The sensitivity of the committed dose coefficients to the uncertainty in the fraction of uranium absorbed into the blood from the alimentary tract is presented in Table 8 for Case I and Case II. The analysis examines the influence of the fraction of absorption (f_A) from the alimentary tract to blood by means of two Monte Carlo simulations. In the first simulation, the f_A parameter was varied while all other parameters were held constant, shown in the 'f_A only' column. Conversely, in the second simulation, all other parameters were varied while f_A was fixed, as

Table 8
Statistical summary of results for the sensitivity analysis of e (50) (Sv/Bq) for the ingestion of U-238: absorption from the alimentary tract.

	All parameters		Particle transport only		f_A only	
	Case I[b]	**Case II**[c]	**Case I**[b]	**Case II**[c]	**Case I**[b]	**Case II**[c]
ICRP value[a]	3.1E-08	3.1E-08	3.1E-08	3.1E-08	3.1E-08	3.1E-08
Mean	4.0E-08	3.8E-08	3.7E-08	3.5E-08	3.4E-08	3.3E-08
Median	3.2E-08	3.1E-08	3.2E-08	3.1E-08	3.1E-08	3.0E-08
GSD	2.0	1.9	1.7	1.7	1.5	1.5
Q_L	8.4E-09	8.5E-09	1.1E-08	1.1E-08	1.4E-08	1.4E-08
Q_U	1.2E-07	1.1E-07	9.2E-08	8.3E-08	6.8E-08	6.6E-08
Mean/ICRP	1.3	1.2	1.2	1.1	1.1	1.1
Median/ICRP	1.0	1.0	1.0	1.0	1.0	1.0
Q_U/ICRP	3.9	3.6	3.0	2.7	2.2	2.1
ICRP/Q_L	3.7	3.6	2.8	2.8	2.2	2.2

GSD: Geometric standard deviation; Q_U: the upper 97.5th percentile; Q_L: the lower 2.5th percentile. Column "Particle transport only" implies only the particle transport parameters in Tables 1 and 2 were varied; "f_A only" implies on the f_A parameter value was varied.

[a] Value taken from ICRP OIR dataviewer (ICRP, 2022).

[b] Study implemented in INTDOSKIT with variation of HATM rates and inclusion of progeny.

[c] Study implemented in INTDOSKIT using the data obtained from Puncher and Burt (2013).

shown in the "Particle transport only" column.

The results show that the mean committed dose coefficients exceed the ICRP reference value in all scenarios, indicating that average doses increase when model uncertainties are taken into account. The median values remain close to the ICRP reference value, indicating that the central tendency of the dose distributions is in good agreement with the ICRP estimate. The greatest variability, indicated by the highest GSD, occurs when all parameters are varied simultaneously. As expected, this variability decreases when only particle transport parameters or only the f_A parameter is varied individually, with the lowest variability observed in the "f_A only" condition, implying that including all parameters introduces the greatest uncertainty, whereas focusing on specific parameters such as f_A reduces it.

The uncertainty range, defined by the lower (Q_L) and upper (Q_U) quantiles, is widest when all parameters are varied, reflecting the highest overall uncertainty. This range narrows when either particle transport parameters or the f_A parameter is considered individually, with the narrowest range seen in the "f_A only" condition. The upper percentiles (Q_U) show significant deviations from the ICRP value when all parameters are considered, indicating higher uncertainty at the upper end. In contrast, the lower percentiles are closer to the ICRP value, especially when only f_A is varied, indicating less uncertainty at the lower end.

Therefore, efforts to reduce the uncertainty in dose assessments should prioritize obtaining more accurate estimates of the f_A parameter, as it has a significant impact on dose variability and uncertainty i.e., accounts for approximately 75% of the uncertainty in committed effective dose coefficient. Although the ICRP value provides a good central estimate, significant variability due to uncertainties in model parameters, especially f_A, needs to be considered in radiological protection and dose assessment. Overall, these results highlight the need to consider the full range of parameter variability to ensure accurate and conservative dose assessments.

3.4. Sensitivity of doses to variation in rates governing turnover of uranium in bone

The sensitivity analysis of the effect of uncertainty in bone turnover rates on the committed effective dose coefficient, e (50) is presented in Table 9. The results in Table 9 show significant differences between Case I and Case II for three parameter variations: "Particle transport only", "Particle transport only (except bone rates)" and "Bone rates only".

For the "Particle transport only" variation, the mean effective dose coefficient for Case I is 3.7E-08 Sv/Bq, slightly higher than the value of 3.5E-08 Sv/Bq for Case II. The medians are close, with 3.2E-08 Sv/Bq for Case I and 3.1E-08 Sv/Bq for Case II respectively. Both cases have a geometric standard deviation (GSD) of 1.7, indicating similar variability in dose estimates. The lower quantile (Q_L) is 1.1E-08 Sv/Bq for both cases, while the upper quantile (Q_U) is 9.2E-08 Sv/Bq for Case I and 8.3E-08 Sv/Bq for Case II, showing a higher uncertainty in the upper range for Case I.

For the "Particle transport only (except bone rates)" scenario, the mean committed effective dose coefficients are 3.6E-08 Sv/Bq for Case I and 3.5E-08 Sv/Bq for Case II, while the medians are 3.1E-08 Sv/Bq for Case I and 3.0E-08 Sv/Bq for Case II. Both cases have a GSD of 1.7, indicating consistent variability. The upper quantile (Q_U) is 9.1E-08 Sv/Bq for Case I and 8.1E-08 Sv/Bq for Case II, indicating a slightly higher uncertainty for Case I.

When only bone rates are varied ("bone rates only"), both Case I and Case II have the same mean committed effective dose coefficient of 3.1E-08 Sv/Bq, with medians of 3.1E-08 Sv/Bq for Case I and 3.0E-08 Sv/Bq for Case II. Both cases have a lower GSD of 1.1, indicating reduced variability. The lower quantile (Q_L) is 2.9E-08 Sv/Bq for both cases and the upper quantile (Q_U) is 3.5E-08 Sv/Bq for both cases. The mean/ICRP and median/ICRP ratios are 1.0 for both cases, and the upper quantile ratio (Q_U/ICRP) is 1.1.

Table 9
Results for the sensitivity analysis of e (50) for the ingestion of U-238: rates of turnover in bone.

	Particle transport only		Particle transport only (except bone rates)		Bone rates only	
	Case I[b]	**Case II[c]**	**Case I[b]**	**Case II[c]**	**Case I[b]**	**Case II[c]**
ICRP value[a]	3.1E-08	3.1E-08	3.1E-08	3.1E-08	3.1E-08	3.1E-08
Mean	3.7E-08	3.5E-08	3.6E-08	3.5E-08	3.1E-08	3.1E-08
Median	3.2E-08	3.1E-08	3.1E-08	3.0E-08	3.1E-08	3.0E-08
GSD	1.7	1.7	1.7	1.7	1.1	1.1
Q_L	1.1E-08	1.1E-08	1.1E-08	1.1E-08	2.9E-08	2.9E-08
Q_U	9.2E-08	8.3E-08	9.1E-08	8.1E-08	3.5E-08	3.5E-08
Mean/ICRP	1.2	1.1	1.2	1.1	1.0	1.0
Median/ICRP	1.0	1.0	1.0	1.0	1.0	1.0
Q_U/ICRP	3.0	2.7	2.9	2.6	1.1	1.1
ICRP/Q_L	2.8	2.8	2.8	2.8	1.1	1.1

GSD: Geometric standard deviation; Q_U: the upper 97.5th percentile; Q_L: the lower 2.5th percentile. Column "Particle transport only" implies only the particle transport parameters in Tables 1 and 2 were varied; "particle transport only (except bone rates)" implies that the particle transport parameter values were varied with the rates from bone surface and bone volume fixed at their ICRP reference values; Column "Bone rates only" implies that the rates from bone surface and bone volume were varied with the other particle transport rates kept at their ICRP reference values.

[a] ICRP OIR dataviewer reference value (ICRP, 2022).

[b] Study implemented in INTDOSKIT with variation of HATM rates and inclusion of progeny.

[c] Study implemented in INTDOSKIT using the data obtained from Puncher and Burt (2013).

The analysis indicates that the greatest variability and uncertainty occur when particle transport parameters are varied, with Case I generally showing slightly higher mean and upper quantile values than Case II. When bone rates are excluded from the variation, the variability and uncertainty remain significant but are slightly reduced. When only bone rates are varied, the variability (GSD) is substantially lower, and the mean and median values align closely with the ICRP reference value, suggesting that bone rate variations alone contribute less to overall dose uncertainty.

When comparing the cases, Case I consistently shows higher mean dose coefficients and upper quantile values than Case II, indicating greater sensitivity to parameter variations in the newer systemic model and the Human Alimentary Tract Model (HATM). The similar GSD values in both cases when particle transport parameters were varied suggest comparable patterns of variability despite the different underlying models. The consistently lower variability in the "bone rates only" condition in both cases indicates that bone turnover rates have a stabilizing effect on the overall dose variability.

For conservative safety assessments, it is prudent to consider the higher means and upper percentiles (Q_U) in the particle transport scenarios, as they reflect potentially higher doses due to uncertainties. The stability of the bone turnover rates, as indicated by the low GSD and narrow percentile range, suggests that these parameters are less critical in contributing to dose variability than the particle transport parameters as a whole. This underlines the importance of accurate characterization of particle transport parameters in order to minimize uncertainties in dose assessment for occupational intake of uranium.

Overall, the analysis demonstrates the critical impact of parameter variability on dose estimates and highlights the nuanced differences between the use of older and newer biokinetic models. These findings are essential for refining radiological protection models and understanding the key drivers of dose variability in occupational settings.

Table 10
Results for the sensitivity analysis of e (50) for the ingestion of U-238 under Case I: HATM rates.

	Particle transport only	Particle transport only (except HATM rates)	HATM rates only
ICRP value[a]	3.1E-08	3.1E-08	3.1E-08
Mean	3.7E-08	3.6E-08	3.2E-08
Median	3.2E-08	3.2E-08	3.1E-08
GSD	1.7	1.7	1.2
Q_L	1.1E-08	1.2E-08	2.1E-08
Q_U	9.2E-08	8.5E-08	4.6E-08
Mean/ICRP	1.2	1.2	1.0
Median/ICRP	1.0	1.0	1.0
Q_U/ICRP	3.0	2.7	1.5
ICRP/Q_L	2.8	2.6	1.5

GSD: Geometric standard deviation; Q_U: the upper 97.5th percentile; Q_L: the lower 2.5th percentile. Column "Particle transport only" implies only the particle transport parameters in Tables 1 and 2 were varied; "particle transport only (except HATM rates)" implies that the particle transport parameter values were varied with the HATM rates fixed at their ICRP reference values; Column "HATM rates only" implies that the HATM rates were varied with the other particle transport rates kept at their ICRP reference values.

[a] ICRP OIR dataviewer reference value (ICRP, 2022).

3.5. Sensitivity of doses to variation in particle transport rates of uranium in HATM

The statistical analysis in Table 10 shows that the "HATM rates only" category aligns more closely with the ICRP reference value in terms of mean, median and dispersion (GSD). It also shows less variability and fewer extreme values (Q_U). This suggests that when considering HATM rates alone, the estimates are more precise and consistent with the ICRP standard. On the other hand, the "Particle transport only" and "Particle transport only (except HATM rates)" categories show higher variability and a tendency to overestimate compared to the ICRP value, indicating less consistency and potential outliers in the data set.

This paper demonstrates the use of INTDOSKIT to study and quantify the uncertainties in the biokinetic model parameters used for the calculation of dose coefficients for the ingestion of U-238 by workers. The analysis calculates committed effective and equivalent dose coefficient distributions that reflect the uncertainty and variability in model parameter values. With 60,000 repetitions, the dataset's convergence was acceptable, as indicated by the GSD-value development of the e (50) distribution.

These distributions were well-fitted by lognormal distributions. The median and range of the committed dose coefficients can infer the uncertainty in the mean e (50) and derive uncertainty factors (UF). The UF values estimate the uncertainty in the dose coefficient's position relative to the corresponding ICRP dose coefficient used in deriving the UF values. Simulation results of the parameter uncertainty analysis can be used to inform the choice of UF values for intake of U-238 by ingestion.

The calculated values for Case I and Case II are quite similar, with Case I values being slightly higher. This can be attributed to the fact that the transfer rates in the upper regions of the HATM are quite fast, so that ingested material passes through these regions in a very short time, resulting in less time for irradiation. Secondly, this study assumed that absorption of ingested material from the alimentary tract into the blood occurs only in the small intestine, as there is no specific information on absorption in other regions of the HATM. Therefore, the use of the HATM published in ICRP Publication 100 results in only minimal differences in dose values compared to those calculated using the GIT model of ICRP Publication 30.

The sensitivity analysis confirms that it is the uncertainty on the value of the f_A parameter that makes the largest single contribution to the uncertainty in the committed effective dose coefficient for ingestion of U-238 particularly by workers. This is evident from the higher GSD and dose ratios in Tables 6 and 7 for Case I and Case II respectively. This observation is not surprising considering that the value of the f_A parameter indicates the fraction of ingested material that reaches the systemic organs and tissues. The ratio of the 97.5th percentile value to e (50) suggests that the uncertainty in the location of the mean dose with respect to the ICRP value should be at least a factor of 2.2.

The results of this study are consistent with those of a previous study by Puncher and Burt, showing comparable GSD values and uncertainty factors, especially in the sensitivity analysis. The only significant difference is in the calculated dose coefficients: 4.5E-08 Sv/Bq (Puncher and Burt, 2013) vs. 3.1E-08 Sv/Bq (ICRP, 2022). Puncher and Burt (2013) used older ICRP publication 60 values for specific equivalent energy (SEE), whereas this study used recent voxel phantoms with radiation-weighted S-coefficients. The authors attribute this discrepancy to differences in the structure of the biokinetic model and the phantoms used. The introduction of uncertainties in the particle transport rates within the HATM in this study (Case I), which was not done by Puncher and Burt, may also contribute to the discrepancy.

It should be noted that this analysis does not account for other uncertainties in internal dose assessment, such as intake estimation from measurement data. Additionally, uncertainties in the dosimetric model, i.e., S-Coefficients, were not included. If distribution data for S-Coefficients or underlying SAF-values become available, their uncertainties could be considered similarly. The authors believe that the biokinetic model contributes more significantly to overall uncertainty than the dosimetric model. Lastly, this study focused solely on ingestion exposure. Future research will consider other exposure routes such as inhalation.

4. Conclusion

This paper demonstrates the effectiveness of INTDOSKIT in quantifying uncertainties in biokinetic model parameters for the calculation of U-238 ingestion dose coefficients. Through an analysis of 60,000 replicates, the study produced dose coefficient distributions that highlight the variability in model parameters and show that while the ICRP reference values are generally reliable, they may underestimate average doses and miss extreme cases. The sensitivity analysis identified the fraction of uranium absorbed from the alimentary tract into the blood (f_A) as a key contributor to uncertainty, emphasizing the need for accurate estimation of this parameter. The study supports the robustness of INTDOSKIT and suggests that while ICRP values are useful, the incorporation of additional statistical measures, such as higher percentiles or the use of the mean as a reference value, could improve radiation protection and dose assessment for U-238 ingestion.

CRediT authorship contribution statement

Thomas Makumbi: Writing – original draft, Visualization, Validation, Software, Methodology, Investigation, Formal analysis, Conceptualization. **Bastian Breustedt:** Writing – review & editing, Supervision, Software, Methodology. **Wolfgang Raskob:** Writing – review & editing, Supervision, Resources, Project administration, Funding acquisition. **Sadeeb Simon Ottenburger:** Writing – review & editing, Supervision, Resources, Project administration, Methodology, Funding acquisition.

Declaration of competing interest

The authors declare that they have no known competing financial interests or personal relationships that could have appeared to influence the work reported in this paper.

Data availability

Data will be made available on request.

Acknowledgements

This work received funding from the Euratom research and training programme 2019–2020 under grant agreement No 900009 (RadoNorm).

References

Agha, A.R., El-Mongy, S.A., Kandel, A.H.T., 2011. Assay of uranium isotopic ratios 234U/238U in bottom sediment samples using destructive and nondestructive techniques (Nasser Lake). In: Proceedings of the 8th Conference on Nuclear and Particle Physics. November 20-24, 2011, Hurghada, Egypt. Available at: https://inis.iaea.org/collection/NCLCollectionStore/_Public/43/099/43099476.pdf.

Aslam, M., 2019. Introducing Kolomogorov-Smirnov tests under uncertainty: an application to radioactive data. ACS Omega Publications 5 (1), 914–917. https://doi.org/10.1021/acsomega.9b03940.

Breustedt, B., Chavan, N., Makumbi, T., 2024. An R-code for calculation of dose coefficients and studying their uncertainties. Health Phys. https://doi.org/10.1097/HP.0000000000001833. https://pubmed.ncbi.nlm.nih.gov/39283588/.

Cardoso, D.O., Galeno, T.D., 2023. Online evaluation of the Kolmogorov-Smirnov test on arbitrarily large samples. Journal of Computational Science 67, 101959. https://doi.org/10.1016/j.jocs.2023.101959.

Ghasemi, A., Zahediasl, S., 2012. Normality tests for statistical analysis. A guide for non-statisticians. Int. J. Endocrinol. Metabol. 10 (2), 486–489. https://doi.org/10.5812/ijem.3505.

Hagel, M.L., Trutzenberg, F., Eid, M., 2024. Applying the robust Chi-squared goodness-of-fit test to multilevel multitrait-multimethod models: a Monte Carlo simulation study on statistical performance. Psychology International 6, 462–491. https://doi.org/10.3390/psycholint6020029.

Heijungs, R., 2020. On the number of Monte Carlo runs in comparative probabilistic LCA. Int. J. Life Cycle Assess. 25 (2), 394–402. https://doi.org/10.1007/s11367-019-01698-4.

ICRP, 1979. Limits on intakes of radionuclides for workers: Part 1. ICRP Publication 30. Ann. ICRP 2 (3–4).

ICRP, 1991. 1990 recommendations of the international commission on radiological protection. ICRP Publication 60. Ann. ICRP 21 (1–3).

ICRP, 1995. Age-dependent doses to members of the public from intake of radionuclides: Part 3. Ingestion dose coefficients. ICRP Publication 69. Ann. ICRP 23 (3).

ICRP, 2006. Human alimentary tract model for radiological protection. ICRP Publication 100. Ann. ICRP 36 (1–2).

ICRP, 2015. Occupational intakes of radionuclides: Part 1. ICRP Publication 130. Ann. ICRP 44 (2).

ICRP, 2017. Occupational intakes of radionuclides: Part 3. ICRP Publication 137. Ann. ICRP 46 (3/4).

ICRP, 2019. Occupational intakes of radionuclides: Part 4. ICRP Publication 141. Ann. ICRP 48 (2/3).

ICRP, 2022. Occupational intakes of radionuclides: Part 5. ICRP Publication 151. Ann. ICRP 51 (1–2).

Khatun, N., 2021. Applications of normality test in statistical analysis. Open J. Stat. 11, 113–122. https://doi.org/10.4236/ojs.2021.111006.

Kreuzer, M., Dufey, F., Laurier, D., Nowak, D., Marsh, J.W., Schnelzer, M., Sogl, M., Walsh, L., 2015. Mortality from internal and external radiation exposure in a cohort of male German uranium millers, 1946-2008. Int. Arch. Occup. Environ. Health 88, 431–441. https://doi.org/10.1007/s00420-014-0973-2.

Kwon, T., Chung, Y., Yoo, J., Ha, W., Cho, M., 2020. Uncertainty quantification of bioassay functions for the internal dosimetry of radioiodine. J. Radiat. Res. 61 (6), 860–870. https://doi.org/10.1093/jrr/rraa081.

Lanzante, J.R., 2021. Testing for differences between two distributions in the presence of serial correlation using the Kolmogorov-Smirnov and Kuiper's tests. Int. J. Climatol. 1–10. https://doi.org/10.1012/joc.7196.

Leggett, R.W., Harrison, J., Phipps, A., 2007. Reliability of the ICRP's dose coefficients for members of the public: IV. Basis of the human alimentary tract model and uncertainties in model predictions. Radiat. Protect. Dosim. 123 (2), 156–170. https://doi.org/10.1093/rpd/ncl104.

Li, W.B., 2018. Internal dosimetry: a review of progress. Health Phys. 53 (2), 72–99. https://doi.org/10.5453/jhps.53.72.

Li, W.B., Gerstmann, U.C., Höllriegl, V., Szymczak, W., Roth, P., Hoeschen, C., Oeh, U., 2009. Radiation dose assessment of exposure to depleted uranium. J. Expo. Sci. Environ. Epidemiol. 19, 502–514. https://doi.org/10.1038/jes.2008.40.

Li, W.B., Roth, P., Wahl, W., Oeh, U., Höllriegl, V., Paretzke, H.G., 2005. Biokinetic modelling of uranium in man after injection and ingestion. Radiat. Environ. Biophys. 44, 29–40. https://doi.org/10.1007/s00411-005-0272-0.

Lopez, M.A., Sierra, I., Hernandez, C., Garcia, S., Garcia, D., Perez, A., 2020. Internal dosimetry of uranium workers exposed during nuclear fabrication process in Spain. Radiat. Phys. Chem. 171, 108706. https://doi.org/10.1016/j.radphyschem.2020.108706.

Luong, A., 2018. Asymptotic results for goodness-of-fit tests using a class of generalized spacing methods with estimated parameters. Open J. Stat. 8, 731–746. https://doi.org/10.4236/ojs.2018.84048.

Ma, M., Wang, R., Xu, L., Xu, M., Liu, S., 2020. Emerging health risks and underlying toxicological mechanisms of uranium contamination: lessons from the past two decades. Environ. Int. 145, 106107. https://doi.org/10.1016/j.envint.2020.106107.

Marsh, J.W., Blanchardon, E., Gregoratto, D., Hofmann, W., Karcher, K., Noßke, D., Tomasek, L., 2012. Dosimetric calculations for uranium miners for epidemiological studies. Radiat. Protect. Dosim. 1–13. https://doi.org/10.1093/rpd/ncr310.

Puncher, M., Burt, G., 2013. The reliability of dose coefficients for inhalation and ingestion of uranium by members of the public. Radiat. Protect. Dosim. 157 (2), 242–254. https://doi.org/10.1093/rpd/nct134.

Puncher, M., Harrison, J.D., 2012. Uncertainty analysis of doses from ingestion of plutonium and americium. Radiat. Protect. Dosim. 148 (3), 284–296. https://doi.org/10.1093/rpd/ncr032.

Rana, R., Singhal, R., 2015. Chi-square test and its application in hypothesis testing. Journal of the Practice of Cardiovascular Sciences 1 (1), 69–71. https://doi.org/10.4103/2395-5414.157577.

Rump, A., Eder, S., Lamkowski, A., Hermann, C., Abend, M., Port, M., 2019. A quantitative comparison of the chemo-and radiotoxicity of uranium at different enrichment grades. Toxicol. Lett. 313, 159–168. https://doi.org/10.1016/j.toxlet.2019.07.004.

Surucu, B., 2008. A power comparison and simulation study of goodness-of-fit tests. Comput. Math. Appl. 56, 1617–1625. https://doi.org/10.1016/j.camwa.2008.03.010.